

# Current status of weak gravitational lensing

Henk Hoekstra<sup>a,b</sup>, H.K.C. Yee<sup>b</sup>, and Michael D. Gladders<sup>b,c</sup>

<sup>a</sup>*CITA, University of Toronto, 60 St. George Street,  
M5S 3H8, Toronto Canada*

<sup>b</sup>*Dept. of Astronomy and Astrophysics, University of Toronto,  
60 St. George Street, M5S 3H8, Toronto Canada*

<sup>c</sup>*Observatories of the Carnegie Institution of Washington,  
813 Santa Barbara Street, Pasadena, California 91101*

---

## Abstract

Weak gravitational lensing of distant galaxies by foreground structures has proven to be a powerful tool to study the mass distribution in the universe. Nowadays, attention has shifted from clusters of galaxies to the statistical properties of the large scale structures and the halos of (field) galaxies. These applications have become feasible with the advent of panoramic cameras on 4m class telescopes.

In this review we will give an overview of recent advances in this fast evolving field of astronomy. We start with a discussion of the recent measurements of weak lensing by large scale structure (“cosmic shear”), which can be used to constrain cosmological parameters. We also show how weak lensing can be used to measure the relation between galaxies and dark matter (galaxy biasing) directly.

Another area that benefitted greatly from the current data is the weak lensing by galaxies (galaxy-galaxy lensing). Weak lensing provides a unique probe of the gravitational potential on large scales. Hence, in the context of dark matter, it can provide constraints on the extent and shapes of dark matter halos. Furthermore, it can test alternative theories of gravity (without dark matter). The best constraint comes from the first detection of the anisotropy of the lensing signal around lens galaxies, which suggest that the dark matter halos are flattened. An isotropic signal, as predicted by MOND, is excluded with 99% confidence.

*Key words:* dark matter, gravitational lensing

---

## 1 Introduction

Weak gravitational lensing is a valuable tool to study the (dark) matter distribution of a range of objects in the universe. The differential deflection of

light rays by intervening structures allows us to study the projected mass distribution of the deflectors, without having to rely on assumptions about the state or nature of the deflecting matter.

In 1984 Tyson et al. tried to detect the weak lensing signal induced by an ensemble of galaxies using photographic plates. However, the first successful detection was made using CCD images of the massive cluster of galaxies A1689 (Tyson et al., 1990). Although much theoretical work concentrated on weak lensing by large scale structure (e.g., Miralda-Escudé, 1991; Blandford et al., 1991; Kaiser, 1992), this area of astronomy blossomed with study of the mass distribution in clusters of galaxies (e.g., Bonnet et al., 1994; Fahlman et al., 1994; Luppino & Kaiser, 1997; Hoekstra et al., 1998, 2000, for an extensive review see Mellier 1999) and galaxy groups (Hoekstra et al., 2001a). These results were an important first step in demonstrating the feasibility of the technique, but nowadays more and more studies concentrate on the “field”.

Adequate schemes to correct for a variety of observational distortions (such as PSF anisotropy, seeing, camera distortion) were developed during the 1990s (e.g., Kaiser et al., 1995; Luppino & Kaiser, 1997; Hoekstra et al., 1998; Kuijken, 1999; Kaiser, 2000; Bernstein & Jarvis, 2002). Together with the development of wide field CCD cameras, these advances allowed for the first detections of weak lensing by large scale structure in the spring of 2000 (Bacon et al., 2000; Kaiser et al., 2000; Van Waerbeke et al, 2000; Wittman et al., 2000).

These first detections were based on small data sets, and consequently the accuracy of the measurements was low. However, the amount of data is increasing rapidly (e.g., Bacon et al., 2002; Maoli et al., 2001; Hoekstra et al., 2002a,b; Refregier et al., 2002; Van Waerbeke et al, 2001a, 2002). Current data sets cover a few to tens of degrees on the sky. Planned surveys, such as the CFHT Legacy Survey, which will obtain deep imaging data for  $170 \text{ deg}^2$  in five filters, will be another major leap forward. The constraints on cosmological parameters are tightening rapidly, and the consistency of the most recent results (Bacon et al., 2002; Hoekstra et al., 2002b; Refregier et al., 2002; Van Waerbeke et al, 2002) suggest that cosmic shear can play an important role in this era of “precision cosmology”.

Another important application of weak lensing is the study of the distribution of the dark matter with respect to the galaxies. For instance, one can study the statistical properties of the galaxy and dark matter distributions: the biasing relations (Hoekstra et al., 2001b, 2002c). Such measurements can provide important constraints on models of galaxy formation. Weak lensing can also be used to study the properties of the dark matter halos surrounding galaxies. Rotation curves of spiral galaxies have provided important evidence for the existence of dark matter halos (e.g., van Albada & Sancisi, 1986). Also,

strong lensing studies of multiple imaged systems require massive halos to explain the observed image separations. However, both methods provide mainly constraints on the halo properties at relatively small radii.

The weak lensing signal can be measured out to large projected distances, and in principle it can be a powerful probe of the potential at large radii, constraining the amount of dark matter (e.g., Brainerd et al., 1996; Griffiths et al., 1996; Dell’Antonio & Tyson, 1996; Hudson et al., 1998; Fischer et al., 2000; Hoekstra, 2000; Wilson et al., 2001; McKay et al., 2001), the extent of the dark matter halos (e.g., Brainerd et al., 1996; Hudson et al., 1998; Fischer et al., 2000; Hoekstra, 2000; Hoekstra et al., 2002d,d) or the average shape of the halos (Hoekstra et al., 2002d).

So far, we have assumed that we can apply the theory of General Relativity to describe gravity. Consequently, the observational data require the existence of dark matter. However, at the large scales probed in this paper, alternative theories have been proposed to explain the shapes of galaxy rotation curves without the use of dark matter. In particular Modified Newtonian Dynamics (MOND; Milgrom (1983)) successfully reproduces rotation curves using only visible matter. Ideally, one would like to test such alternative theories far away from the visible matter. Potentially, weak lensing can place tight constraints on such theories (Mortlock & Turner, 2001a,b).

In this review, we will address various applications of, and recent developments in weak gravitational lensing. In Section 2 we concentrate on the cosmic shear measurements, and Section 3 deals with galaxy biasing. The constraints on the halos of galaxies from weak lensing are described in Section 4. In Section 5 we discuss how the lensing data can be used to place limits on alternative theories of gravity.

Throughout the paper we will make use of results based on  $R_C$ -band imaging data from the Red-Sequence Cluster Survey (RCS; Gladders & Yee, 2000; Yee & Gladders, 2001). We refer the reader to Hoekstra et al. (2002a) for a thorough discussion of the weak lensing analysis of these data.

## 2 Lensing by large scale structure

The measurement of the coherent distortions of the images of faint galaxies caused by weak lensing by intervening large scale structures provides a direct way to study the statistical properties of the growth of structure in the universe. Compared to many other methods, weak lensing probes the matter directly, regardless of the light distribution. In addition it provides measurements on scales from the quasi-linear to the non-linear regime where compar-

isons between observations and predictions are still limited.

We provide a basic description of the theory of weak lensing by large scale structure. Detailed discussions on this subject can be found elsewhere (e.g., Schneider et al., 1998; Bartelmann & Schneider, 2001). Current measurements of cosmic shear have concentrated on the two-point statistics, which can be related to the convergence power spectrum, which is defined as

$$P_\kappa(l) = \frac{9H_0^4\Omega_m^2}{4c^4} \int_0^{w_H} dw \left( \frac{\bar{W}(w)}{a(w)} \right)^2 P_\delta \left( \frac{l}{f_K(w)}; w \right), \quad (1)$$

where  $w$  is the radial (comoving) coordinate,  $w_H$  corresponds to the horizon,  $a(w)$  the cosmic scale factor, and  $f_K(w)$  the comoving angular diameter distance. As shown by Jain & Seljak (1997) and Schneider et al. (1998) it is necessary to use the non-linear power spectrum in equation (1). This power spectrum is derived from the linear power spectrum following the prescriptions from Peacock & Dodds (1996). We note that this approach might not be accurate enough for future measurements (e.g., Van Waerbeke et al, 2001b, 2002).

$\bar{W}(w)$  is the source-averaged ratio of angular diameter distances  $D_{ls}/D_s$  for a redshift distribution of sources  $p_b(w)$ :

$$\bar{W}(w) = \int_w^{w_H} dw' p_b(w') \frac{f_K(w' - w)}{f_K(w')}. \quad (2)$$

Hence, it is important to know the redshift distribution of the sources, in order to relate the observed lensing signal to  $P_\kappa(l)$ .

Until recently, the top-hat variance was the most widely used two-point statistic. It is related to the convergence power spectrum through

$$\langle \gamma^2 \rangle(\theta) = 2\pi \int_0^\infty dl l P_\kappa(l) \left[ \frac{J_1(l\theta)}{\pi l\theta} \right]^2, \quad (3)$$

where  $\theta$  is the radius of the aperture used to compute the variance, and  $J_1$  is the first Bessel function of the first kind.

Another useful statistic is the aperture mass, which is defined as (e.g., Kaiser et al., 1994; Schneider et al., 1998)

$$M_{\text{ap}}(\theta) = \int d^2\phi U(\phi) \kappa(\phi). \quad (4)$$

Provided  $U(\phi)$  is a compensated filter, i.e.,  $\int d\phi \phi U(\phi) = 0$ , with  $U(\phi) = 0$  for  $\phi > \theta$ , the aperture mass can be expressed in term of the observable tangential shear  $\gamma_t$  using a different filter function  $Q(\phi)$  (which is a function of  $U(\phi)$ ). Using the choice of filter functions from Schneider et al. (1998), the variance of the aperture mass  $\langle M_{\text{ap}}^2 \rangle$  is related to the power spectrum through

$$\langle M_{\text{ap}}^2 \rangle = 2\pi \int_0^\infty dl l P_\kappa(l) \left[ \frac{12}{\pi(l\theta)^2} J_4(l\theta) \right]^2, \quad (5)$$

where  $J_4$  is the fourth-order Bessel function of the first kind. The measurement of  $\langle M_{\text{ap}}^2 \rangle$  is of particular interest, because the measurements at different scales are only weakly correlated.

The first detections of cosmic shear (Bacon et al., 2000; Kaiser et al., 2000; Maoli et al., 2001; Van Waerbeke et al., 2000; Wittman et al., 2000) actually computed the excess variance in apertures directly from the data. Some more recent studies have used the same technique (Bacon et al., 2002; Hoekstra et al., 2002a; Refregier et al., 2002; Van Waerbeke et al., 2001a).

However, recent studies show that an optimal use of the data is to measure the shear correlation functions from the data (Pen et al., 2002; Van Waerbeke et al., 2002; Hoekstra et al., 2002b). These correlation functions can be related to the various two-point statistics (Crittenden et al., 2002; Pen et al., 2002). In addition, this approach allows one to split the signal into two components: an “E”-mode, which is curl-free, and a “B”-mode, which is sensitive to the curl of the shear field. Gravitational lensing arises from a gravitational potential, and hence it is expected to produce a curl-free shear field. Thus, the “B”-mode can be used to quantify the level of systematics involved in the measurement. The decomposition is naturally carried out by using the aperture mass statistic  $M_{\text{ap}}$ .

Several sources of B-mode have been identified. For instance, simple models describing the intrinsic alignments of galaxies predict a small B-mode (e.g., Crittenden et al., 2002), although the amplitude is still uncertain. Hence, any measured B-mode is dominated by residual systematics in the data (e.g., imperfect correction of the PSF anisotropy) or intrinsic alignments. The effect of intrinsic alignments can be minimized by selecting galaxies with a broad redshift distribution. In future surveys, with photometric redshift information for the galaxies, the contribution from intrinsic alignments can be removed completely by correlating the shapes of galaxies with different redshifts.

Figure 1 shows the results of such a decomposition into “E” and “B”-modes. The analysis, which is described in detail in Hoekstra et al. (2002b), uses 53 deg<sup>2</sup> of RCS imaging data. For all three samples we find that the “B”-mode

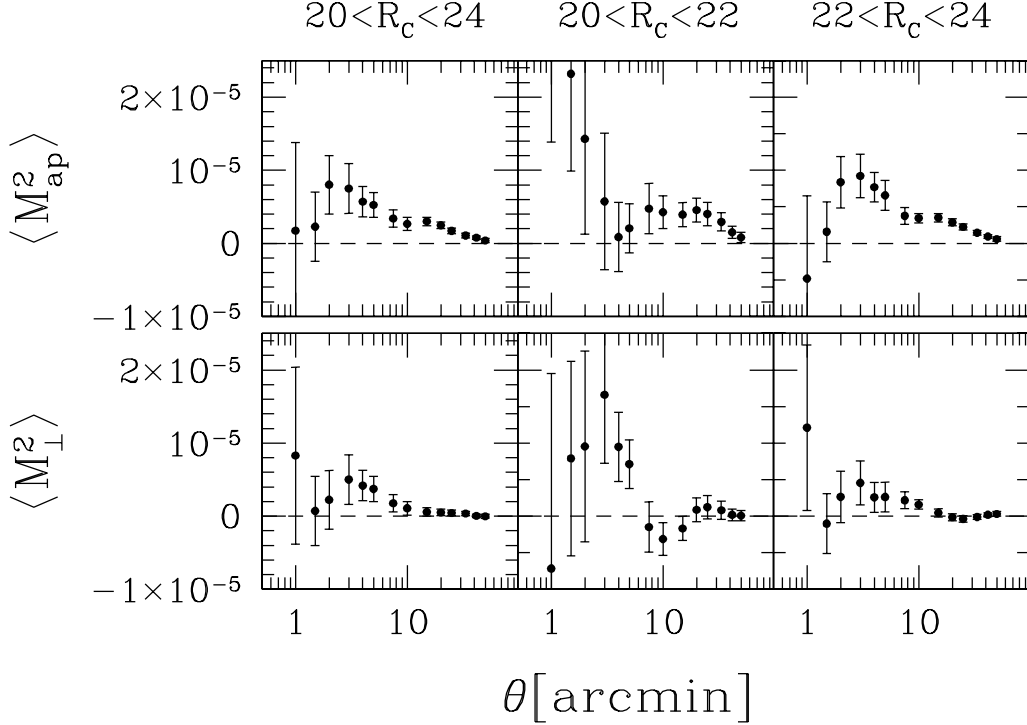


Fig. 1. The upper panels show the measured variance of the aperture mass  $\langle M_{\text{ap}}^2 \rangle$  as a function of aperture size  $\theta$  for different samples of source galaxies. This signal corresponds to the E-mode. The lower panels show the variance  $\langle M_{\perp}^2 \rangle$  when the phase of the shear is increased by  $\pi/2$ , and corresponds to the B-mode. The error bars indicate the  $1\sigma$  statistical uncertainty in the measurements, and have been derived from the field-to-field variation of the 13 RCS patches (thus the error bars include cosmic variance). Note that the points are slightly correlated. We detect a significant B-mode on scales 5 – 10 arcminutes. On scales larger than 10 arcminutes the B-mode vanishes. The sample of bright galaxies ( $20 < R_C < 22$ ) should not be affected significantly by systematics because their sizes are large compared to the PSF. Therefore the significant B-mode at scales of a few arcminutes is likely to be caused by intrinsic alignments. To minimize the effect of intrinsic alignments on our cosmological parameter estimation, we will use the sample of galaxies with  $22 < R_C < 24$  to this end.

(lower panels) vanishes on scales larger than  $\sim 10$  arcminutes, suggesting that neither observational distortions or intrinsic alignments of sources have corrupted our measurements.

On smaller scales we detect a significant “B”-mode. Interestingly, we detect a significant signal for the bright galaxies ( $20 < R_C < 22$ ). These galaxies have sizes that are large compared to the PSF, and therefore they are less affected by residual systematics. Intrinsic alignments are expected to be particularly important for these bright galaxies, and we therefore conclude that (at least part of) the observed “B”-mode is likely to be caused by intrinsic alignments.

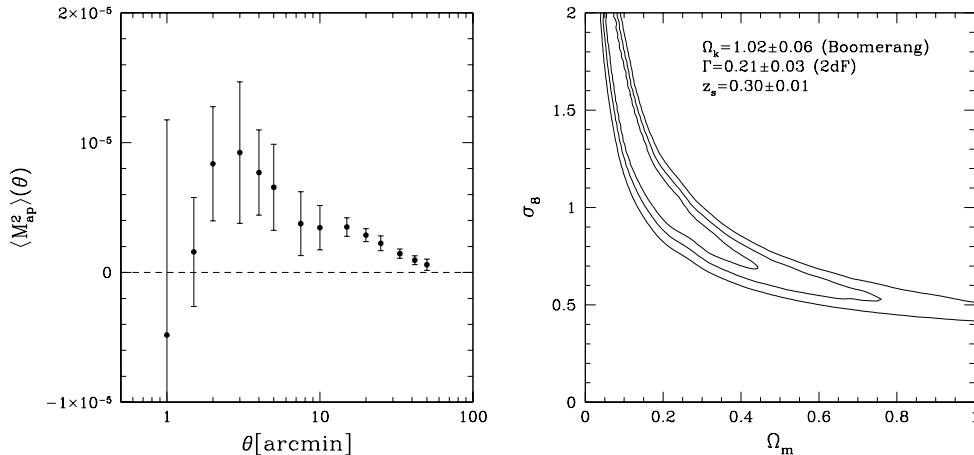


Fig. 2. *Left panel:* The measured variance of the aperture mass  $\langle M_{\text{ap}}^2 \rangle$  as a function of aperture size  $\theta$  for source galaxies with  $22 < R_C < 24$ . The error bars have been increased to account for the unknown correction for the “B”-mode observed in Figure 1. *Right panel:* Constraints on  $\Omega_m$  and  $\sigma_8$  using priors Gaussian priors on  $\Gamma$ ,  $\Omega_{\text{tot}} = \Omega_m + \Omega_\Lambda$ , and the source redshift distribution  $z_s$  (which gives  $\langle z \rangle = 0.59 \pm 0.02$ ). The likelihood contours have been derived by comparing the measurements to CDM models with  $n = 1$ . For  $\Gamma$  we used the constraints from the 2dF survey  $\Gamma = 0.21 \pm 0.03$  (Peacock et al., 2001; Efstathiou et al., 2001), and for  $\Omega_{\text{tot}}$  we used the Boomerang constraints  $\Omega_{\text{tot}} = 1.02 \pm 0.06$  (Netterfield et al., 2001). The contours indicate the 68.3%, 95.4%, and 99.7% confidence limits on two parameters jointly.

The next step is to relate the observed signal to estimates of cosmological parameters. Our current understanding of the redshift distribution of the source galaxies is sufficient to obtain accurate constraints. The most accurate results are derived when one uses external priors on the parameters. Useful constraints come from redshift surveys and the temperature fluctuations in the CMB. Current weak lensing measurements provide joint constraints on  $\Omega_m$  and  $\sigma_8$ , and Figure 2 shows the results from Hoekstra et al. (2002b). However, measurements of higher order statistics, such as the skewness, can be used to break the degeneracies between  $\Omega_m$ , and  $\sigma_8$  (e.g., Van Waerbeke et al., 1999). Recently the first detection of a measure of skewness was reported (Bernardeau et al., 2002a,b), and the prospects for measurements of higher order statistics are good.

In Table 1 we list the estimates of  $\sigma_8$  (for  $\Omega_m = 0.3$  and  $\Gamma = 0.21$ ) as derived by the most recent weak lensing surveys (Bacon et al., 2002; Hoekstra et al., 2002b; Refregier et al., 2002; Van Waerbeke et al., 2002). Despite the fact that these results have been obtained using a wide variety of telescopes (both ground based and HST), filters, and integration times, the agreement is remarkable.

We note that the value of  $\sigma_8$  determined from the RCS data is essentially

Cosmic shear survey	$\sigma_8$
Hoekstra et al. (2002b) (RCS)	$0.86^{+0.04}_{-0.05}$
Bacon et al. (2002)	$0.97^{+0.10}_{-0.09}$
Refregier et al. (2002)	$0.94 \pm 0.14$
Van Waerbeke et al (2002)	$0.98 \pm 0.06$

Table 1

Values of  $\sigma_8$  and 68% confidence intervals as derived from 4 independent cosmic shear measurements (adopting  $\Omega_m = 0.3$ ,  $\Omega_\Lambda = 0.7$ , and  $\Gamma = 0.21$ ).

constrained by the measurements at scales larger than 10 arcminutes, where the “B”-mode is negligible. The result from Van Waerbeke et al. (2002) might be biased high, because of their large scale “B”-mode. Both Bacon et al. (2002) and Refregier et al. (2002) do not separate their signal into “E” and “B”-modes, and therefore it might also include some residual systematics.

A widely used method to determine the normalization of the power spectrum uses the number density of rich clusters of galaxies (e.g., Borgani et al., 2001; Carlberg et al., 1997; Eke et al., 1996; Fan & Bahcall, 1998; Pen, 1998a; Pierpaoli et al., 2001; Reiprich & Böhringer, 2001; Seljak, 2001; Viana et al., 2001). Such systems are rare, and as a result a very sensitive probe of  $\sigma_8$ , provided one can determine their mass. The derived values for  $\sigma_8$  from this technique range from values as low as  $0.61 \pm 0.05$  (Viana et al., 2001) to values around unity (e.g., Fan & Bahcall, 1998; Pen, 1998a; Pierpaoli et al., 2001). The statistical error bars on most of these measurements are small, and hence the large spread in values suggests an underlying large systematic uncertainty.

### 3 Galaxy biasing

The growth of structures in the universe via gravitational instability is an important ingredient in our understanding of galaxy formation. However, the connection to observations is not straightforward, as we need to understand the relation between the dark matter distribution and the galaxies themselves. Galaxy formation is a complex process, and it is not guaranteed a priori that this relation, referred to as galaxy biasing, is a simple one. The bias might be non-linear, scale dependent or stochastic. In the simplest case, linear, deterministic biasing, the relation between the dark matter and the galaxies can be characterized by a single number  $b$  (e.g., Kaiser, 1987).

Most observational constraints of biasing come from dynamical studies (see Strauss & Willick, 1995) which probe relatively large scales ( $10h_{50}^{-1}$  Mpc or more). Recent estimates on these scales suggest values of  $b \sim 1$  for  $L_*$  galaxies



(e.g., Peacock et al., 2001; Verde et al., 2001). On smaller scales some constraints come from measurements of the galaxy two-point correlation function, which is compared to the (dark) matter correlation function computed from numerical simulations. These studies indicate that the bias parameter  $b \simeq 0.7$  on scales less than  $\sim 2h_{50}^{-1}$  Mpc ( $\Omega_m = 0.3$ ,  $\Omega_\Lambda = 0.7$ ). On larger scales  $b$  increases to a value close to unity (Jenkins et al., 1998) Although this procedure provides useful information about the bias parameter  $b$  as a function of scale, it does rely on the assumptions made for the numerical simulations. In addition, it cannot be used to examine how tight the correlation between the matter and light distribution is. To do so, we need to measure the galaxy-mass cross-correlation coefficient  $r$ , which is a measure of the amount of stochastic and non-linear biasing (e.g., Pen, 1998b; Dekel & Lahav, 1999; Somerville et al., 2001).

Redshift surveys can be used to determine the relative values of  $b$  and  $r$  for different galaxy types (Tegmark & Bromley, 1999; Blanton, 2000), but weak gravitational lensing provides the only direct way to measure the galaxy-mass cross-correlation function (e.g., Fischer et al., 2000; Wilson et al., 2001; McKay et al., 2001; Hoekstra et al., 2001b). Fischer et al. (2000) used the SDSS commissioning data to measure the galaxy-mass correlation function and their results suggested an average value of  $b/r \sim 1$  on submegaparsec scales. This approach has been explored by Guzik & Seljak (2001) who used semi-analytic models of galaxy formation combined with N-body simulations. Their results suggest that the cross-correlation coefficient is close to unity.

To study the galaxy biasing we use a combination of the galaxy and mass auto-correlation functions, as well as the cross-correlation function. A common definition of the “bias” parameter is the ratio of the variances of the galaxy and dark matter densities, which is the definition we will use here. In the case of deterministic, linear biasing the galaxy density contrast  $\delta_g$  is simply related to the mass density contrast  $\delta$  as  $\delta_g = b\delta$  (Kaiser, 1987), and the ratio of the variances is the only relevant parameter. However, the bias relation is likely to be more complicated as it depends on the process of galaxy formation, and might be stochastic, non-linear or both. We allow for non-linear stochastic biasing by including the galaxy-mass cross-correlation coefficient  $r$  (e.g., Pen, 1998b; Dekel & Lahav, 1999; Somerville et al., 2001). The cross-correlation coefficient  $r$  mixes non-linear and stochastic effects (Dekel & Lahav, 1999; Somerville et al., 2001) which we currently cannot disentangle with weak lensing.

The bias parameters are related to the observed correlation functions through (Hoekstra et al., 2002c)

$$b^2 = f_1(\theta_{\text{ap}}, \Omega_m, \Omega_\Lambda) \times \frac{\langle N^2(\theta_{\text{ap}}) \rangle}{\langle M_{\text{ap}}^2(\theta_{\text{ap}}) \rangle}, \quad (6)$$

and

$$r = f_2(\theta_{\text{ap}}, \Omega_m, \Omega_\Lambda) \times \frac{\langle M_{\text{ap}}(\theta_{\text{ap}})N(\theta_{\text{ap}}) \rangle}{\sqrt{\langle N^2(\theta_{\text{ap}}) \rangle \langle M_{\text{ap}}^2(\theta_{\text{ap}}) \rangle}}, \quad (7)$$

where  $f_1$  and  $f_2$  depend on the assumed cosmological model and the redshift distributions of the lenses and the sources (see Van Waerbeke, 1998; Hoekstra et al., 2002c). The values of  $f_1$  and  $f_2$ , however, depend minimally on the assumed power spectrum and the angular scale.

There is no reason for  $b$  or  $r$  to be constant with scale, but as long as  $b$  and  $r$  vary slowly with scale, we can still infer the bias parameters from Eqs. (3) and (4). The  $M_{\text{ap}}$  statistic is sensitive to a fairly small range in  $k$  in Fourier space for a given aperture size. If the galaxy power spectrum  $P_{\text{gg}}(k)$  can be related to the matter power spectrum  $P_{\text{mm}}(k)$  through  $P_{\text{gg}}(k) = b^2(k)P_{\text{mm}}(k)$ , we essentially measure the average value of  $b(k)$  in the  $k$ -range probed by the  $M_{\text{ap}}$  statistic (Van Waerbeke, 1998; Hoekstra et al., 2002c). In other words,  $M_{\text{ap}}$  is a pass-band filter, which also explains why different scales are only slightly correlated (Schneider et al., 1998).

Hoekstra et al. (2002c) studied the bias properties of galaxies with  $19.5 < R_C < 21$ . They combined the weak lensing measurements from the RCS and the VIRMOS-DESCART survey (e.g., Van Waerbeke et al, 2002) to obtain the first direct measurements of the bias parameter  $b$  and the galaxy-mass cross-correlation coefficient  $r$  as a function of scale (with scales ranging from 0.1 to  $4 h^{-1}$  Mpc). The results of this analysis are presented in Figure 3. Hoekstra et al. (2002c) find that both  $b$  and  $r$  vary with scale for this sample of galaxies. The low value of  $r$  on scales  $\sim 0.5 - 1 h^{-1}$  Mpc suggests significant stochastic biasing and/or non-linear biasing. Although both  $b$  and  $r$  vary with scale, the ratio  $b/r$  turns out to be almost constant with scale. Hoekstra et al. (2002c) find that  $b/r = 1.090 \pm 0.035$  out to  $7 h^{-1}$  Mpc.

Models of galaxy formation predict the relation between the galaxies and the underlying dark matter distribution. The two commonly used approaches are hydrodynamic simulations (e.g., Blanton et al., 2000; Yoshikawa et al., 2001) or (e.g., Kauffmann et al., 1999a,b; Somerville et al., 2001; Guzik & Seljak, 2001). A comparison of the models with the lensing results can provide accurate constraints. Unfortunately, current models of galaxy formation are limited to relatively bright (i.e., massive) galaxies, because of the mass resolution of the numerical simulations. Most of the galaxies in the sample studied by Hoekstra et al. (2002c) are too faint to be included in the simulations. This severely limits a direct comparison. However, with available multi-color data the weak lensing results can be matched better to the models, and vice versa, future models should include lower mass galaxies.

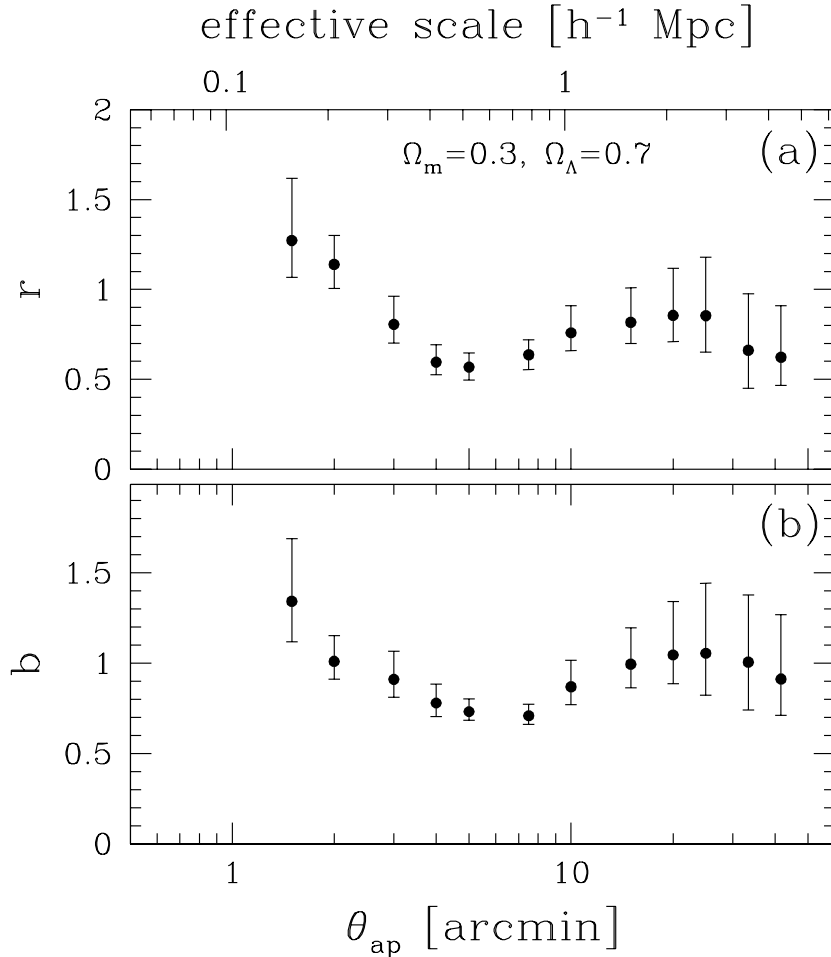


Fig. 3. (a) The measured value of the galaxy-mass cross correlation coefficient  $r$  as a function of scale for the  $\Lambda$ CDM cosmology. (b) The bias parameter  $b$  as a function of scale. The upper axis indicates the effective physical scale probed by the compensated filter at the median redshift of the lenses ( $z = 0.35$ ). The error bars correspond to the 68% confidence intervals. Note that the measurements at different scales are slightly correlated.

#### 4 Constraints on the halos of galaxies

Rotation curves of spiral galaxies (e.g., van Albada & Sancisi, 1986) and strong lensing analyses of multiple imaged sources have provided strong evidence for the existence of massive dark matter halos around galaxies. However, the lack of visible tracers hampers our knowledge of the gravitational potential at large projected distances. Only satellite galaxies (e.g., Zaritsky & White, 1994) provide a way to probe the outskirts of isolated galaxy halos.

However, the weak gravitational lensing signal induced by such galaxies can be measured out to large projected distances, thus providing a powerful probe of the potential at large radii, which can be used to study the extent of the

dark halos (e.g., Brainerd et al., 1996; Hudson et al., 1998; Fischer et al., 2000; Hoekstra, 2000; Hoekstra et al., 2002d,d).

The lensing signal induced by an individual galaxy is too low to be detected, and one has to study the ensemble averaged signal around a large number of lenses. Early measurements of the galaxy-galaxy lensing signal were limited by the small number of lenses/sources (e.g., Brainerd et al., 1996; Hudson et al., 1998), because of the lack of panoramic cameras. Recently the accuracy with which the lensing signal can be measured has improved significantly. Fischer et al. (2000) measured a very significant signal, and Wilson et al. (2001) studied the signal around early type galaxies as a function of redshift. McKay et al. (2001) used the redshift information from the SDSS to study the galaxy-galaxy lensing signal as a function of galaxy properties.

Here we present some preliminary results based on 45 deg<sup>2</sup> of RCS  $R_C$  band data. The detailed analysis is described in Hoekstra et al. (2002d), and a description of the method can be found in Hoekstra (2000). We use galaxies with  $19.5 < R_C < 21$  as lenses, and galaxies with  $21.5 < R_C < 24$  as sources which are used to measure the lensing signal. The simplest approach to galaxy-galaxy lensing is to measure the ensemble averaged tangential distortion as a function of radius around the sample of lenses. The result for our data is presented in Figure 4a. The signal when the phase of the shear is increased by  $\pi/2$  is presented in Figure 4b. This signal is consistent with zero, indicating that observational systematics have been successfully corrected for.

We fit a SIS model to the tangential distortion which yields  $\langle r_E \rangle = 0''.129 \pm 0''.011$ . Given the redshifts of the lenses and the sources this corresponds to a velocity dispersion of  $\langle \sigma^2 \rangle^{1/2} = 123 \pm 5$  km/s. The corresponding circular velocity can be obtained using  $V_c = \sqrt{2}\sigma$ .

The tangential shear profile is a convolution of the actual halo profile around galaxies and the clustering properties of the lenses. Fischer et al. (2000) used this tangential shear profile, taking into account the clustering of the lenses, to obtain constraints on the extent of the dark matter halos surrounding the lenses. They conclude that the halos are large, but they were unable to obtain tight constraints. In Section 4.1 we show the results of a maximum likelihood analysis of the data, and demonstrate that this approach gives much better constraints on the sizes of halos.

An application of galaxy-galaxy lensing that is still in its early stage is the measurement of the shapes of galaxy halos. If the halos are flattened, the lensing signal will be slightly anisotropic. Provided the halos and the galaxies are aligned, we can measure this angular dependence of the tangential shear. In Section 4.2, we present the first results of such an analysis.

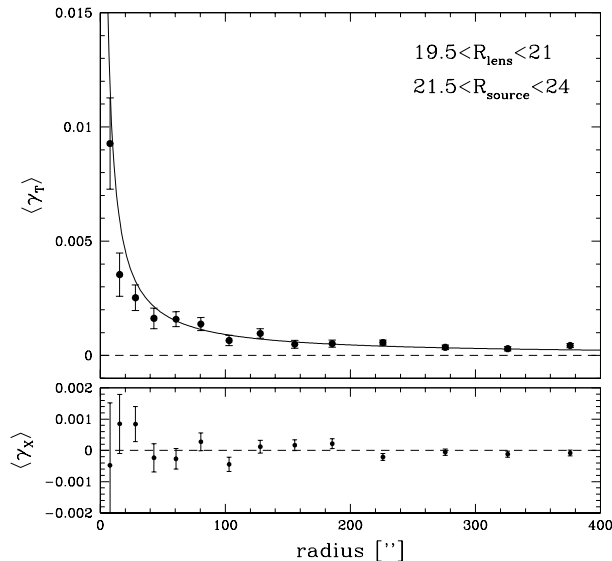


Fig. 4. (a) The ensemble averaged tangential distortion as a function of radius around the sample of lens galaxies. The measurements have been corrected for the presence of source galaxies associated with the lens galaxies. (b) The signal when the phase of the distortion is increased by  $\pi/2$ : no signal should be present if the signal in (a) is due to lensing. The vertical error bars indicate the  $1\sigma$  errors

#### 4.1 Sizes of galaxy halos

For an isolated lens, the induced lensing signal is purely tangential. This is no longer the case for an ensemble of lenses (which also cluster): the other lenses cause small perturbations, and the shear is no longer tangential. To study the sizes of halos around galaxies Fischer et al. (2000) used only the tangential component. However, Hoekstra (2000) was able to obtain better constraints using a maximum likelihood analysis on their imaging data of CNOC2 fields. The maximum likelihood analysis uses a parameterized model for the mass distribution of individual galaxies is compared to the data. This has the advantage that one uses the information contained in both components of the distortion. It implicitly assumes that all clustered dark matter is associated with galaxies. Furthermore, the contributions from faint neighboring galaxies are not included in the model, and as such, the results reflect the average density profile around the lenses.

A useful model to describe a truncated halo is (Schneider & Rix, 1997; Hoekstra, 2000)

$$\Sigma(r) = \frac{\sigma^2}{2Gr} \left( 1 - \frac{r}{\sqrt{r^2 + s^2}} \right), \quad (8)$$

where  $s$  is a measure of the truncation radius (i.e., the scale where the pro-

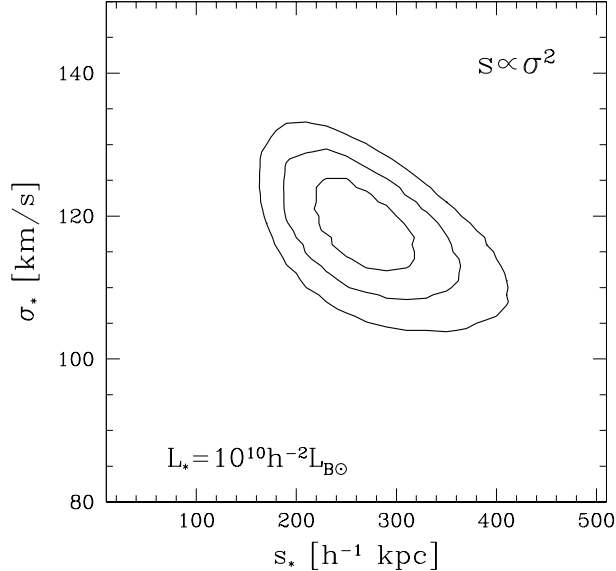


Fig. 5. Likelihood contours for the velocity dispersion  $\sigma_*$  and truncation parameter  $s_*$  of a galaxy with a fiducial luminosity  $L_* = 10^{10} h^{-2} L_{B\odot}$ . To derive this result we assumed that the velocity dispersion  $\sigma$  scales  $\propto L_B^{1/4}$ , and that the truncation parameter  $s$  scales  $\propto L_B^{1/2}$  (or  $\propto \sigma^2$ ). The contours indicate the 68.3%, 95.4%, and the 99.7% confidence on two parameters jointly.

file steepens). The total mass of this model is finite, and half of the mass is contained with  $r = \frac{3}{4}s$ .

As before we assume that  $\sigma \propto L_B^{1/4}$ . We also have to assume a scaling relation for the truncation parameter  $s$ . Currently, no such observational constraints exist, although galaxy-galaxy lensing analyses with redshifts for the lenses can be used to this end. As shown by Hoekstra (2000) different scaling relations lead to somewhat different values for  $s$ . Also one can compare the predictions from N-body simulations (Navarro et al., 1997) to the data. The aim here is not to derive the definitive value of  $s$ , but to demonstrate that weak lensing can constrain the “extent” of the dark matter halos.

Currently, we do not have (photometric) redshift information for the lens galaxies in the RCS fields. To derive constraints on the dark matter halos we follow Hoekstra (2000), and make mock catalogs of lenses where the redshifts are drawn from the CNOC2 redshift survey (Yee et al., 2000) on the basis of their  $R_C$ -band magnitude. This provides a very crude redshift estimate. We found that the derived results did not change much between realisations.

In the analysis we assumed that the velocity dispersion  $\sigma$  scales  $\propto L_B^{1/4}$ , and that the truncation parameter  $s$  scales  $\propto L_B^{1/2}$  (or  $\propto \sigma^2$ ). Figure 5 shows the results of maximum likelihood analysis for a galaxy with a fiducial luminosity of  $L_* = 10^{10} h^{-2} L_{B\odot}$ . For such a galaxy we find  $\sigma_* = 118_{-4}^{+5}$ , in fair agreement with other estimates. In addition, the average extent of the dark matter halo

is well constrained, and we obtain  $s_* = 265_{-25}^{+33}h^{-1}$  kpc, and a 99.7% confidence upper limit of  $s_* < 390h^{-1}$  kpc.

## 4.2 Shapes of galaxy halos

Numerical simulations of cold dark matter result in triaxial halos, with typical ellipticity of  $\sim 0.3$  (e.g., Dubinski & Carlberg, 1991). In the context of collisionless cold dark matter, the theoretical evidence for flattened halos is quite strong. However, the observational evidence is still limited. Sackett (1999) gives an overview of current constraints which probe the vertical potential on scale  $\leq 15$  kpc. These results suggest an average value of  $c/a = 0.5 \pm 0.2$  (where  $c/a$  is the ratio of the shortest to longest principle axis of the halo).

Current constraints are mainly limited by the lack of visible tracers that can probe the gravitational potential around galaxies. Hence, galaxy-galaxy lensing is potentially the most powerful way to derive constraints on the average shape of dark matter halos. As such, it provides an important test of the collisionless cold dark matter paradigm. Brainerd & Wright (2000) and Natarajan & Refregier (2000) examined the data requirements needed for a detection of the halo flattening. Although their estimates appear to be too optimistic, it is clear that large amounts of data are required. The measurement of the average shape of the dark matter halos is much more difficult than the previous measurements: the galaxy-galaxy lensing signal is small, and now one needs to measure an even smaller azimuthal variation. Furthermore one has to assume that the galaxy and its halo are aligned, which appears to be a reasonable assumption.

Our approach is different from that of Brainerd & Wright (2000) and Natarajan & Refregier (2000), who propose to study the azimuthal variation in the tangential shear around the lenses. Instead we use a maximum likelihood analysis to derive constraints on the shapes of dark matter halos. We note that this is a first attempt to do so, and more detailed work is required. We simply assume that the (projected) ellipticity of the dark matter halo is related to the shape of the galaxy as  $e_{\text{halo}} = fe_{\text{lens}}$ , and use the best fit parameters for the velocity dispersion and truncation. The ellipticities of the lenses have been corrected for the PSF, similar to the sources. The lensing signal is dominated by the contribution from early type galaxies, and therefore our parameterisation of the halo shape is reasonable.

The resulting  $\Delta\chi^2$  as a function of  $f$  is presented in Figure 6. The main conclusion from this analysis is that spherical halos are excluded with 99% confidence. Although the inferred ellipticity of dark matter halos depends on the adopted dependence on the light distribution, we note that the exclusion

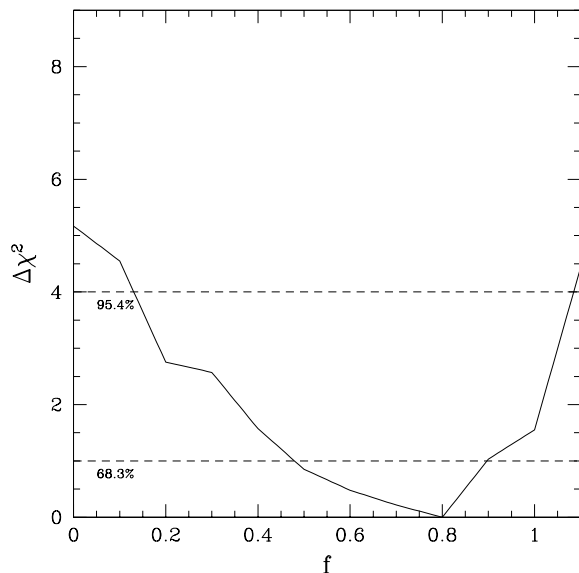


Fig. 6.  $\Delta\chi^2$  as a function of  $f$ . We have assumed that the ellipticity of the halos is related to the observed ellipticity of the lens as  $e_{\text{halo}} = f e_{\text{lens}}$ . We have indicated the 68.3% and 95.4% confidence intervals. Round halos ( $f = 0$ ) are excluded with 99% confidence. The average ellipticity of the galaxies is  $\langle e_{\text{lens}} \rangle = 0.261$  and hence the average halo ellipticity is  $\langle e_{\text{halo}} \rangle = 0.21^{+0.02}_{-0.08}$  (68.3% confidence), which corresponds to an average projected axis ratio of  $c/a = 0.65^{+0.12}_{-0.02}$  (68.3% confidence).

of a spherical halo is robust. Compared to the measurement of the tangential shear as a function of radius, the result presented here is more sensitive to residual systematics. A detailed analysis, however, demonstrates that our result is robust, and not caused by systematics.

The average ellipticity of the lens galaxies is  $\langle e_{\text{lens}} \rangle = 0.261$ . The best fit value of  $f = 0.8$  then implies a average projected halo ellipticity of  $\langle e_{\text{halo}} \rangle = 0.21^{+0.02}_{-0.08}$  (68.3% confidence), which corresponds to an projected axis ratio of  $c/a = 0.65^{+0.12}_{-0.02}$  (68.3% confidence). Although the weak lensing yields a projected axis ratio, the result is in fair agreement with the numerical simulations. We note, however, that it is not straightforward to interpret this result: the lensing signal comes from a range of galaxy types, although typically the lensing signal is dominated by the early type galaxies, for which our halo model might be appropriate.

## 5 Limits on alternative theories of gravity

In the context of General Relativity, we have to invoke large amounts of dark matter to explain a wide variety of observational results. However, at the large scales probed in this paper, no definite tests of general relativity have been



made, and alternative theories of gravity have been proposed to explain the shapes of galaxy rotation curves without the use of dark matter. In particular Modified Newtonian Dynamics (MOND; Milgrom (1983)) successfully reproduces rotation curves using only visible matter.

Dynamical studies can provide useful constraints on such theories, but only in the regions where there is visible matter. The best regime to test such alternative theories is far away from the visible matter. This requires a way to probe the gravitational potential on large physical scales. Weak gravitational lensing is currently the best approach to this end. As shown above, it can accurately probe the gravitational potential on scales where other methods fail. In addition, in the absence of dark matter halos, galaxy-galaxy lensing is simple, because the galaxies can be treated as point masses. Unfortunately most alternative theories of gravity do not provide a useful description of gravitational lensing. For instance, MOND lacks a relativistic theory that can describe light deflection.

To test alternative theories of gravity we can use two different approaches. A measurement of the radial dependence of the lensing signal gives the best accuracy, but it requires knowledge of the deflection law. The most direct test is the detection of the azimuthal variation of the lensing signal around the lenses: alternative theories predict an isotropic lensing signal, and the measurement does not require knowledge of the deflection law!

In alternative theories of gravity, any anisotropy in the lensing signal caused by the intrinsic shapes of the galaxies (i.e., the light and gas distribution) decreases  $\propto r^{-2}$ , and hence is negligible on the scales probed here. Therefore the observed anisotropy in the galaxy-galaxy lensing signal (see Section 4.2) poses a serious problem for alternative theories of gravity. More detailed work is required to confirm this result, but new data sets will provide much better constraints in the very near future, and allow us to study the anisotropy a function of projected distance from the galaxy.

The detection of the anisotropy of the lensing signal around galaxies provides the best evidence for the existence of dark matter halos around galaxies. For completeness we also discuss constraints on the radial dependence of gravity, following the approach suggested by Mortlock & Turner (2001b).

### *5.1 Constraints on the radial dependence of light deflection*

Mortlock & Turner (2001b) considered a “zero-th” order approach, by recalling that the deflection angle in GR is twice the Newtonian value. They simply assumed that a similar relation holds for MOND, and derive the “deflection law”. We note, however, that this approach is rather simplistic, and ad hoc,

because the force law used by Mortlock & Turner (2001b) does not return to the Newtonian form on large scales (although with a modified gravitational constant), which is required from general considerations (e.g., Sanders, 1986; Walker, 1994; White & Kochanek, 2001).

The aim of this section is to give an indication of the potential of current data sets for the purpose of testing alternative theories of gravity. Along this line of reasoning, we first concentrate on the general class of models considered by Mortlock & Turner (2001a). One simply starts from the deflection law for a point mass. In General Relativity, the deflection law is

$$\alpha(\theta) = -\frac{\theta_E^2}{\theta}, \quad (9)$$

where  $\theta_E$  is the Einstein radius of the lens. The Einstein radius depends on the mass  $M$  of the lens and the angular diameter distances from observer to lens ( $D_l$ ), observer to source ( $D_s$ ), and lens to source ( $D_{ls}$ ):

$$\theta_E = \sqrt{\frac{4GM}{c^2} \frac{D_s}{D_l D_{ls}}}. \quad (10)$$

Hence, another complication of lensing in alternative theories of gravity arises because it is not clear how the angular diameter distances vary with redshift. However, this uncertainty should only affect the amplitude of the lensing signal, and not its angular dependence.

Mortlock & Turner (2001a) considered a generic deflection law, which is parameterized as

$$\alpha(\theta) = -\frac{\theta_E^2}{\theta} \left( \frac{\theta_0}{\theta + \theta_0} \right)^{\xi-1}. \quad (11)$$

For  $\theta \ll \theta_0$ , this deflection law reduces to the usual deflection, as is the case for  $\xi = 1$ . For large  $\theta$  the deflection angle decreases  $\propto \theta^{-\xi}$ . The case of  $\xi = 0$ , can be considered as the approximate MOND deflection angle.

It is straightforward to relate the deflection angle to the observable shear. For this particular choice of deflection angle we obtain (Mortlock & Turner, 2001a)

$$\gamma(\theta) = \frac{\theta_E^2}{\theta_0 \theta^2} \left( \frac{\xi + 1}{2} \theta + \theta_0 \right) \left( \frac{\theta_0}{\theta + \theta_0} \right)^\xi. \quad (12)$$

Mortlock & Turner (2001a) compared this model to the observed ensemble averaged tangential shear around galaxies in the SDSS (Fischer et al., 2000).

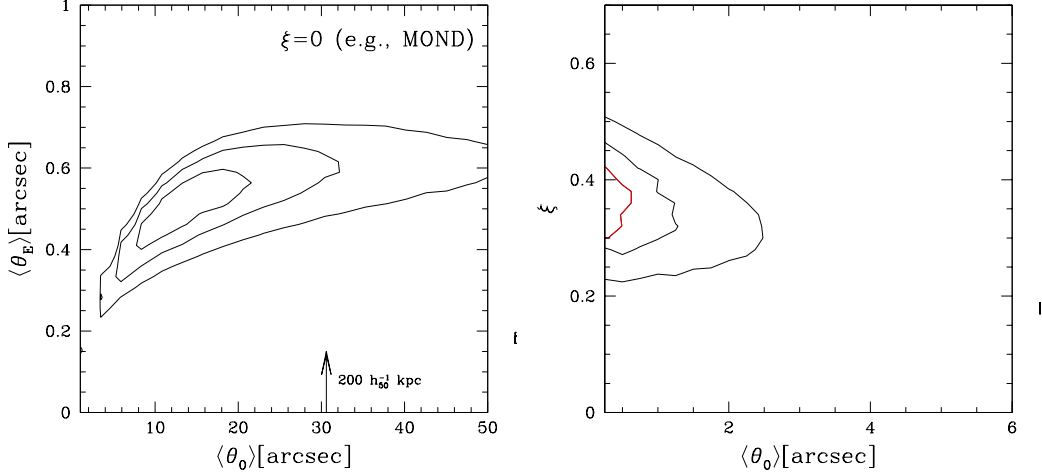


Fig. 7. *Left panel:* Likelihood contours for  $\xi = 0$ , which can be considered as a good approximation to the MOND case. The contours indicate the 68.3%, 95.4% and 99.7% confidence limits on two parameters jointly. The allowable range for the value of  $\theta_0$  excludes small values: the MOND regime sets in at too large physical scales. The best fit value for the Einstein radius corresponds to a mass-to-light ratio of  $M/L_B = 1.5M_\odot/L_{B\odot}$ . *Right panel:* The likelihood contours for the parameters  $\xi$  and  $\theta_0$  as determined from a maximum likelihood analysis of 16 deg<sup>2</sup> of RCS  $R_C$  band imaging data. The results have been marginalized over the Einstein radius  $\theta_E$ . As expected,  $\xi = 1$  (GR without dark matter) is ruled out. Also the best fit of  $\xi = 0.1$  from Mortlock & Turner (2001a) is ruled out with high confidence. In addition, the maximum likelihood solution is much worse than the GR + truncated halo model presented in section 4, and the current data are sufficient to rule out models of gravity with deflection laws given by equation 11 at the  $10\sigma$  confidence level.

They found a best fit value of  $\xi = -0.1$  and  $\theta_0 = 3.7$  arcsecond. As a result, Mortlock & Turner (2001a) concluded the MOND “predictions” are consistent with the SDSS measurements.

However, as we will show now, a maximum likelihood analysis can provide much better constraint. As before, we use the measurements from the RCS. We now treat the lenses as point masses with the deflection law given by equation 11.

Figure 7 shows the results of a maximum likelihood analysis of 16 deg<sup>2</sup> of  $R_C$  band imaging data from the RCS. The left panel shows the constraints on  $\theta_0$  and  $\theta_E$  for  $\xi = 0$  (i.e., the “MOND” approximation). The allowable range for the value of  $\theta_0$  excludes small values: the MOND regime sets in at too large physical scales. The best fit value for the Einstein radius corresponds to a mass-to-light ratio of  $M/L_B = 1.5M_\odot/L_{B\odot}$ , which is similar to what one would expect from the stars themselves. The right panel of Figure 7 shows the constraints on  $\theta_0$  and  $\xi$  when we marginalize over  $\theta_E$ . Both the  $\xi = 1$

(GR without dark matter) and the  $\xi = 0$  case (“MOND”) are excluded by the current data.

Comparison of the maximum likelihood solution to the best fit “GR + truncated dark matter halo” model shows that the latter is a much better fit. The results from the “truncated dark matter halo” model indicate that the data favor a model in which the projected mass distribution has a profile that is  $\propto 1/r$  on small scales, and steepens on larger scales. This explains why the  $\xi = 0$  model results in large values of  $\theta_0$ , and why the data favor a value of  $\xi \sim 0.35$ : the best fit model is a compromise between the  $1/r$  and  $1/r^2$  profiles, reflecting the change in slope in the density profile. Comparison of the likelihoods of the deflection law models given by equation 11 and the “truncated halo” model shows that the former models are excluded at the  $10\sigma$  confidence level.

The problems with the deflection laws considered by Mortlock & Turner (2001a) arise because of the form of the deflection law on large scales. As mentioned above, the law of gravity has to return to the  $1/\theta$  form on large scales, and consequently, such theories should not only specify a scale where the effect of alternative gravity becomes important, but also large scale  $\theta_{\text{out}}$ , where the theory returns to “normal” gravity.

To allow for such a scale, we modify the Mortlock & Turner (2001a) deflection law (for  $\xi = 0$ , i.e., the “MOND” case) to

$$\tilde{\alpha}(\theta) = -\frac{\theta_{\text{E}}^2}{\theta\theta_0} \left( \theta + \theta_0 - \frac{\theta^2}{\theta + \theta_{\text{out}}} \right), \quad (13)$$

which gives a shear

$$\tilde{\gamma}(\theta) = \frac{\theta_{\text{E}}^2}{\theta_0\theta^2} \left[ \frac{\theta}{2} + \theta_0 - \frac{\theta^3}{2(\theta + \theta_{\text{out}})^2} \right], \quad (14)$$

For  $\theta \gg \theta_{\text{out}}$  this modified deflection law leads to a deflection angle (or shear) that is a factor  $\theta_{\text{out}}/\theta_0$  times the GR value. Hence, the ratio  $\theta_{\text{out}}/\theta_0$  is a measure of the “mass discrepancy”. Comparison with the truncated halo model shows that both profiles are nearly identical on scales larger than a few  $\theta_0$ , provided the truncation parameter  $s = \theta_{\text{out}}$ . We find that such a model provides a good fit to the data. However, we note that the introduction of  $\theta_{\text{out}}$  is rather ad hoc.

The study of the radial dependence of the deflection law is potentially useful when it is predicted completely by the theory. The ad hoc approach used here can fit the data, and hence gives inconclusive results. As mentioned above, the azimuthal variation of the lensing signal around galaxies provides a more

robust method. The detection of an anisotropic lensing signal poses a serious problem for alternative theories of gravity.

## 6 Conclusions

Weak gravitational lensing has shown tremendous progress in the last few years, thanks mainly to the fact that large areas of the sky can now be observed with wide field cameras, such as the CFH12k camera on CFHT. In this review we have highlighted some of the most recent results.

The most recent cosmic shear studies (Bacon et al., 2002; Hoekstra et al., 2002b; Refregier et al., 2002; Van Waerbeke et al., 2002) show excellent agreement. This is remarkable, given the fact that the data have been taken with different instruments, filters, and depths. These most recent results demonstrate that weak lensing by large scale structure can play an important role in the era of precision cosmology.

Weak lensing provides a direct measure of the (dark) matter distribution on all scales, and hence it is one of the most powerful probes of the relation between the galaxies and the underlying mass distribution. As a result, it provides a direct way to determine the bias parameter  $b$  and the galaxy-mass cross-correlation coefficient  $r$  as a function of scale, on scales not accessible by other techniques. The results obtained by Hoekstra et al. (2002c) suggest significant non-linear or stochastic biasing on scales  $0.5 - 1h^{-1}$  Mpc. These measurements provide important observational constraints on models of galaxy formation.

The lack of visible tracers hampers our knowledge of the gravitational potential around galaxies at large projected radii. Weak lensing has proven to be a powerful tool to probe the extent and shapes of dark matter halos. The maximum likelihood analysis of RCS data indicates a clear steepening of the mass distribution on scales larger than  $\sim 250h^{-1}$  kpc (Hoekstra et al., 2002d). Furthermore, the data allowed for the first detection of the flattening of dark matter halos, with spherical halos excluded at the 99% confidence level.

Finally weak lensing can be used to constrain alternative models of gravity (without dark matter). Ad hoc approaches to study the radial dependence of the deflection law remain inconclusive, mainly because of the lack of predictions. These theories, however, predict an essentially isotropic lensing signal around galaxies, irrespective of the actual deflection law. The detection of an anisotropic lensing signal around galaxies therefore poses a serious problem for theories of alternative gravity, such as MOND.

The main results discussed in this review were obtained in the last few years.

The progress made in such a small amount of time suggests that exciting times are ahead, when even larger data sets become available.

HH thanks the organizers for the invitation to an interesting meeting.

## References

- van Albada, T.S., & Sancisi, R. 1986, *Phil. Trans.*, 320, 447
- Bacon, D., Refregier, A., & Ellis, R.S. 2000, *MNRAS*, 325, 1065
- Bacon, D., Massey, R., Refregier, A., & Ellis, R. 2002, *MNRAS*, submitted, astro-ph/0203134
- Bartelmann, M., & Schneider, P. 2001, *Physics Reports*, 340, 291
- Bernardeau, F., Mellier, Y., & van Waerbeke, L. 2002a, *A&A*, in press, astro-ph/0201032
- Bernardeau, F., van Waerbeke, L., & Mellier, Y. 2002a, *A&A*, submitted, astro-ph/0201029
- Bernstein, G.M. & Jarvis, M. 2002, *AJ*, 123, 583
- Blandford, R.D., Saust, A.B., Brainerd, T.G., & Villumsen, J.V. 1991, *MNRAS*, 251, 600
- Blanton, M. 2000, *ApJ*, 544, 63
- Blanton, M., Cen, R., Ostriker, J.P., Strauss, M.A., & Tegmark, M. 2000, *ApJ*, 531, 1
- Bonnet, H., Mellier, Y., & Fort, B. 1994, *ApJ*, 427, L83
- Borgani, S., et al. 2001, *ApJ*, 561, 13
- Brainerd, T.G, Blandford, R.D., & Smail, I. 1996, *ApJ*, 466, 623
- Brainerd, T.G. & Wright, C.O. 2000, astro-ph/0006281
- Carlberg, R. G., Morris, S. L., Yee, H. K. C., Ellingson, E. 1997, *ApJ*, 479, L19
- Crittenden, R.G., Natarajan, P., Pen, U.-L., & Theuns, T. 2002, *ApJ*, in press, astro-ph/0012336
- Dekel, A., & Lahav, O. 1999, *ApJ*, 520, 24
- Dell’Antonio, I.P., & Tyson, J.A. 1996, *ApJ*, 473, L17
- Dubinski, J. & Carlberg, R.G. 1991, *ApJ*, 378, 496
- Efstathiou G., et al. 2001, *MNRAS*, submitted, astro-ph/0109152
- Eke, V.R., Cole, S., Frenk, C.S. 1996, *MNRAS*, 282, 263
- Gladders, M.D., & Yee, H.K.C. 2000, to appear in “The New Era of Wide-Field Astronomy”, astro-ph/0011073
- Griffiths, R.E., Casertano, S., Im, M., & Ratnatunga, K.U. 1996, *MNRAS*, 282, 1159
- Guzik, J., & Seljak, U. 2001, *MNRAS*, 321, 439
- Fahlman, G., Kaiser, N., Squires, G., & Woods, D. 1994, *ApJ*, 437, 56
- Fan & Bahcall 1998, *ApJ*, 504, 1
- Fischer, P., et al. 2000, *AJ*, 120, 1198

- Hoekstra, H. 2000, PhD thesis, University of Groningen,  
<http://www.ub.rug.nl/eldoc/dis/science/h.hoekstra/thesis.pdf>
- Hoekstra, H., Franx, M., Kuijken, K., & Squires, G. 1998, *ApJ*, 504, 636
- Hoekstra, H., Franx, M., Kuijken, K. 2000, *ApJ*, 532, 88
- Hoekstra, H., Franx, M., Kuijken, K., Carlberg, R.G., Yee, H.K.C., Lin, H.,  
 Morris, S.L., Hall, P.B., Patton, D.R., Sawicki, M., & Wirth, G.D. 2001a,  
*ApJ*, 548, L5
- Hoekstra, H., Yee, H.K.C., & Gladders, M.D. 2001b, *ApJ*, 558, L11
- Hoekstra, H., Yee, H.K.C., Gladders, M.D., Barrientos, L.F., Hall, P.B., &  
 Infante, L. 2002a, *ApJ*, in press
- Hoekstra, H., Yee, H.K.C., & Gladders, M.D. 2002b, *ApJ*, submitted
- Hoekstra, H., van Waerbeke, L., Gladders, M.D., Mellier, Y., & Yee, H.K.C.  
 2002c, *ApJ*, submitted
- Hoekstra, H., Franx, M., Kuijken, K., Carlberg, R.G., & Yee, H.K.C 2002d,  
 in preparation
- Hoekstra, H., Yee, H.K.C., & Gladders, M.D. 2002d, in preparation
- Hudson, M.J., Gwyn, S.D.J., Dahle, H., & Kaiser, N. 1998, *ApJ*, 503, 531
- Jain, B. & Seljak, U. 1997, *ApJ*, 484, 560
- Jenkins, A., Frenk, C.S., Pearce, F.R., Thomas, P.A., Colberg, J.M. et al.  
 1998, *ApJ*, 499, 20
- Kaiser, N. 1987, *MNRAS*, 227, 1
- Kaiser, N. 1992, *ApJ*, 388, 272
- Kaiser, N., Squires, G., Fahlman, G. G., & Woods, D. 1994, in “Clusters of  
 Galaxies”, eds. Durret, Mazure, Tran Thanh Van
- Kaiser, N., Squires, G., & Broadhurst, T. 1995, *ApJ*, 449, 460
- Kaiser, N. 2000, *ApJ*, 537, 555
- Kaiser, N., Wilson, G., & Luppino, G.A. 2000, *ApJL*, submitted, astro-  
 ph/0003338
- Kauffmann, G., Colberg, J.M., Diaferio, A., White, S.D.M. 1999a, *MNRAS*,  
 303, 188
- Kauffmanm, G., Colberg, J.M., Diaferio, A., White, S.D.M. 1999b, *MNRAS*,  
 307, 529
- Kuijken, K. 1999, *A&A*, 352, 355
- Luppino, G.A., & Kaiser, N. 1997, *ApJ*, 475, 20
- Maoli, R., Van Waerbeke, L., Mellier, Y., Schneider, P. Jain, B., Bernardeau,  
 F., Erben, T. & Fort, B. 2001, *A&A*, 368, 766
- McKay, T.A., et al. 2001, *ApJ*, submitted, astro-ph/0108013
- Mellier, Y. 1999, *ARA&A*, 37, 127
- Miralda-Escudé, J. 1991, *ApJ*, 380, 1
- Milgrom, M. 1983, *ApJ*, 270, 365
- Mortlock, D.J., & Turner, E.L. 2001, *MNRAS*, 327, 552
- Mortlock, D.J., & Turner, E.L. 2001, *MNRAS*, 327, 557
- Natarajan, P. & Refregier, A. 2000, *ApJ*, 538, L113
- Navarro, J.F., Frenk, C.S., & White, S.D.M. 1997, *ApJ*, 490, 493
- Netterfield, C.B. et al. 2001, astro-ph/0104460

- Peacock, J.A. & Dodds, S.J. 1996, MNRAS, 780, L19
- Peacock, J.A. et al. 2001, Nature, 410, 169
- Pen, U.-L. 1998, ApJ, 504, 60
- Pen, U.-L. 1998, ApJ, 504, 601
- Pen, U.-L., van Waerbeke, L., Mellier, Y. 2002, ApJ, 567, 31
- Pierpaoli, E., Scott, D., & White, M. 2001, MNRAS, 325, 77
- Schneider, P. 1998, ApJ, 498, 43
- Refregier, A., Rhodes, J., & Groth, E.J. 2002, ApJL, submitted, astro-ph/0203131
- Reiprich, T.H. & Böhringer, H. 2001, astro-ph/0111285
- Sackett, P. 1999 in *Galaxy Dynamics*, ASP Conf. Series 182, eds. D.R. Merritt, M. Valluri, & J.A. Sellwood
- Sanders, R.H. 1986, MNRAS, 223, 539
- Schneider, P., & Rix, H.-W. 1997, ApJ, 474, 25
- Schneider, P. 1998, ApJ, 498, 43
- Schneider, P., van Waerbeke, L., Jain, B., Kruse, G. 1998, MNRAS, 296, 873
- Seljak, U. 2001, MNRAS, submitted, astro-ph/0111362
- Somerville, R.S., Lemson, G., Sigad, Y., Dekel, A., Kauffmann, G., & White, S.D.M. 2001, MNRAS, 320, 289
- Strauss, M.S., & Willick, J.A. 1995, Phys. Rep., 261, 271
- Tegmark, M., & Bromley, B.C. 1999, ApJ, 518, L69
- Tyson, J.A., Valdes, F., Jarvis, J.F., & Mills, A.P., Jr. 1984, ApJ, 281, 59
- Tyson, J.A., Wenk, R.A., & Valdes, F. 1990, ApJ, 349, L1
- van Waerbeke, L. 1998, A&A, 334, 1
- van Waerbeke, L., Bernardeau, F., & Mellier, Y. 1999, A&A, 342, 15
- van Waerbeke, L., et al. 2000, A&A, 358, 30
- van Waerbeke, L., et al. 2001a, A&A, 374, 757
- van Waerbeke, L., Hamana, T., Scoccimarro, R., Colombi, S., Bernardeau, F. 2001b, MNRAS, 322, 918
- van Waerbeke, L., Mellier, Y., Pello, R., Pen, U.-L., McCracken, H.J., Jain, B. 2002, A&A, submitted, astro-ph/0202503
- Verde, L. et al. 2001, MNRAS, submitted, astro-ph/0112161
- Viana, P.T.P., Nichol, R.C., Liddle, A.R. 2001, ApJL, submitted, astro-ph/0111394
- Walker, M.A. 1994, ApJ, 430, 463
- White, M., & Kochanek, C.S. 2001, ApJ, 560, 539
- Wilson, G., Kaiser, N., Luppino, G.A. 2001, ApJ, 556, 601
- Wittman, D.M., Tyson, J.A., Kirkman, D., Dell’Antonio, I., & Bernstein, G. 2000, Nature, 405, 143
- Yee, H.K.C. et al. 2000, ApJS, 129, 475
- Yee, H.K.C., & Gladders, M.D. 2001, in “AMiBA 2001: High-z Clusters, Missing Baryons, and CMB Polarization”, ASP Conference Series, Eds. L.-W. Chen et al., astro-ph/0111431
- Yoshikawa, K., Taruya, A., Jing, Y.P., & Suto, Y. 2001, ApJ, 558, 520
- Zaritsky, D., & White, S.D.M. 1994, ApJ, 435, 599